

AFOSR-Taiwan Nanoscience Initiative

Project Final Report

Project Title

Development of GaN/AlGaIn Terahertz Quantum Cascade Laser

FA4869- 07-1-4076

(AOARD-074076)

Period : September 1, 2007- August 31, 2008

Principal Investigator

Professor S. C. Wang

Institution

Institute of Electro-Optical Engineering,
National Chiao Tung University
1001 Ta Hsueh Road, Hsinchu, TAIWAN 30010
Phone: +886-3-5712121 extension 56320
Fax: +886-3-5716631
Email: scwang@mail.nctu.edu.tw

November 19, 2008

Report Documentation Page

Form Approved
OMB No. 0704-0188

Public reporting burden for the collection of information is estimated to average 1 hour per response, including the time for reviewing instructions, searching existing data sources, gathering and maintaining the data needed, and completing and reviewing the collection of information. Send comments regarding this burden estimate or any other aspect of this collection of information, including suggestions for reducing this burden, to Washington Headquarters Services, Directorate for Information Operations and Reports, 1215 Jefferson Davis Highway, Suite 1204, Arlington VA 22202-4302. Respondents should be aware that notwithstanding any other provision of law, no person shall be subject to a penalty for failing to comply with a collection of information if it does not display a currently valid OMB control number.

1. REPORT DATE 20 NOV 2008		2. REPORT TYPE FInal		3. DATES COVERED 14-06-2007 to 13-06-2008	
4. TITLE AND SUBTITLE Development of GaN-Based Terahertz Quantum Cascade Laser				5a. CONTRACT NUMBER FA48690714076	
				5b. GRANT NUMBER	
				5c. PROGRAM ELEMENT NUMBER	
6. AUTHOR(S) Shing-Chung Wang				5d. PROJECT NUMBER	
				5e. TASK NUMBER	
				5f. WORK UNIT NUMBER	
7. PERFORMING ORGANIZATION NAME(S) AND ADDRESS(ES) National Chiao Tung University,1001 Ta Hsueh Rd,Hsinchu 30010,Taiwan,TW,30010				8. PERFORMING ORGANIZATION REPORT NUMBER N/A	
9. SPONSORING/MONITORING AGENCY NAME(S) AND ADDRESS(ES) AOARD, UNIT 45002, APO, AP, 96337-5002				10. SPONSOR/MONITOR'S ACRONYM(S) AOARD	
				11. SPONSOR/MONITOR'S REPORT NUMBER(S) AOARD-074076	
12. DISTRIBUTION/AVAILABILITY STATEMENT Approved for public release; distribution unlimited					
13. SUPPLEMENTARY NOTES					
14. ABSTRACT This reports research on GaN-based optoelectronic materials and light emitting devices using the MOCVD system for epitaxial growth.					
15. SUBJECT TERMS Quantum Dots, Laser Physics					
16. SECURITY CLASSIFICATION OF:			17. LIMITATION OF ABSTRACT Same as Report (SAR)	18. NUMBER OF PAGES 21	19a. NAME OF RESPONSIBLE PERSON
a. REPORT unclassified	b. ABSTRACT unclassified	c. THIS PAGE unclassified			

1. Introduction

The solid-state coherent source in the terahertz (THz) range has been developed and demonstrated recently using semiconductor materials such as GaAs/AlGaAs material system and AlInAs/GaInAs material system in a quantum cascade laser (QCL) scheme. These THz quantum cascade lasers have so far been operating at less than 150 K. A major obstacle for achieving higher temperature operation is attributed to the thermal excitation of electrons from the ground state into the lower laser state at higher temperatures that reduces the population inversion between the laser states. For GaAs/AlGaAs QCLs, the energy separation between the lower laser state and the ground state where the majority of electrons reside is just above the LO-phonon energy (~ 36 meV), which is comparable to room temperature $k_B T$ (~ 26 meV). Therefore, a material system with larger LO-phonon energy will be desirable for the high-temperature operation of THz QCLs. The GaN-based material system with large LO-phonon energy (~ 90 meV) has been proposed for THz QCLs. The advantages are threefold. First, the large LO-phonon energy in a GaN-based system can reduce the thermal population of the lower laser state. Second, ultra fast LO-phonon scattering in GaN/AlGaN quantum wells can be used for the rapid depopulation of the lower laser state. Third, the large LO-phonon energy can also increase the lifetime of the upper laser state by reducing the relaxation of electrons with higher in-plane kinetic energy via emission of a LO-phonon. Therefore it has been considered the most desirable candidate for far infrared intersubband emission laser. However the GaN material growth technology is still being developed and there is no GaN substrate available yet.

Hexagonal GaN and AlN semiconductors, and AlGaN alloys, have attracted considerable attention due to their successful applications in the fabrication of high-performance electronic and optoelectronic devices, such as heterostructure field-effect

transistors, ultra-violet light-emitting diodes, and laser diodes. By varying the alloy composition, different electrical and optical properties can be obtained in a wide spectral range from 3.4 to 6.3 eV. Our research group has been conducting research on GaN based optoelectronic materials and light emitting devices for past several years using the MOCVD system for epitaxial growth of GaN based materials and structures [1], [2]. Previously, we have grown the GaN/AlGa_N active region for terahertz quantum cascade lasers using MOCVD system based on the quantum cascade structure proposed by Prof. Greg Sun and Dr. Richard Soref, as shown in Fig. 1 [3], [4]. In this year's program with AFOSR, our effort has been focused on the study of composition dependence of optical phonon energies in Al_xGa_{1-x}N alloys by performing Fourier transform infrared reflectance (FTIR) measurements. The phonon energy is vital to the proper performance of the GaN QCL as we mentioned previously. The variation of phonon energy with Al composition we observed needed to be analyzed. Furthermore, to improve the epitaxial layer thickness control of the MOCVD grown GaN/AlGa_N quantum confined structures we have investigated the new growth method of atomic layer deposition (ALD). In previous study, we have established the growth conditions for obtaining good surface morphology of the epitaxial structures and the growth of active layer structure. We also conducted investigation and analysis of the grown structure to establish the compositional contents and thickness of the grown active layer structures which are very important parameters for growth of the overall GaN QCL structure. The research was conducted in collaboration with Prof. Greg Sun of University of Massachusetts Boston and Dr. Richard Soref of AF Hanscom Lab and the results obtained during this period have been published in Journal of Crystal Growth in November 2006. In this final report, we summarize our investigation results and accomplishments in these key areas.

2. Results and Accomplishments

2.1 Growth and characterization of single AlGa_xN epilayer

For all samples, a normal 30-nm-thick GaN nucleation layer was deposited at 500 °C. Before growing a 0.4- μm -thick Al_xGa_{1-x}N film, a 2- μm -thick GaN buffer layer was grown on the GaN nucleation layer. All the growth conditions of GaN buffer layers were the same. Al_xGa_{1-x}N epilayers in composition range of $0 < x < 0.3$ were grown in N₂ and H₂ mixture ambient gas and at pressure of 100 Torr. For the composition range of $0.3 < x < 1$, the Al_xGa_{1-x}N epilayers were grown in N₂ and H₂ mixture ambient gas and at pressure of 50 Torr in order to obtain a better aluminum incorporation efficiency [5]. For the AlN epilayers, in order to obtain better crystal quality, the samples were grown in a pure N₂ ambient gas and at pressure of 100 Torr. The growth process was in-situ monitored by a filmetrics F-series thin-film measurement system. The surface morphology and the exact compositional contents of the GaN/Al_xGa_{1-x}N epitaxial structure are very important factors in the realization of the GaN/AlGa_xN QCL structure. We have grown the AlGa_xN epilayers on sapphire to investigate their morphologies and aluminum compositions in previous study. In order to further engineer these alloys and related optoelectronic devices, it is necessary to work on the fundamental properties of these materials. The infrared optical response of these alloys is important for the determination of crystal quality and phonon properties. Furthermore, composition dependence of optical phonon energies in Al_xGa_{1-x}N alloys are studied by performing Fourier transform infrared reflectance measurements. In QCL structures, electrons scatter from intersubband energy levels by rapidly emitting phonons. Therefore, the study of composition-dependent phonon energies in Al_xGa_{1-x}N alloys is very important in order to understand the dynamic properties and design high performance GaN-based QCLs. Fig. 2 shows a schematic diagram of the AlGa_xN layer with a GaN buffer on the

sapphire (0001) substrate. In order to investigate the phonon frequencies of GaN and $\text{Al}_x\text{Ga}_{1-x}\text{N}$ epilayers on sapphire substrates, it is necessary to obtain the knowledge of the dielectric function for sapphire substrate and identify the influences from sapphire phonon modes. The infrared dielectric anisotropy and phonon modes of sapphire are completely studied by Schubert *et al.* using infrared spectroscopic ellipsometry [6]. They determined the ordinary and extraordinary infrared complex dielectric functions as well as all infrared-active phonon modes of single crystal *c*-sapphire for wavelengths from 3 to 30 μm . In this study, we directly applied all physical parameters of *c*-sapphire including two high-frequency dielectric constants, four distinct infrared-active modes with dipole-moment oscillation perpendicular to the *c* axis, and two modes with dipole-moment oscillation parallel to the *c* axis from the reported values by Schubert *et al.*. These lattice vibrations are split into longitudinal and transversal optical modes due to coulomb interaction. Fig. 3 shows the experimental infrared reflectance spectrum (dotted line) and calculated reflectance spectrum (solid line) by employing the physical parameters of *c*-sapphire from Table 1. It is found that the calculated infrared reflectance spectrum of *c*-sapphire is in good agreement with the experimental result. Since the sapphire substrates are commercial available and stable in crystal quality, we do not numerically fit the measured reflectance spectrum of sapphire in this study. Fig. 4 and 5 show the optical function within the infrared spectral range for the ordinary (solid lines) and the extraordinary (dotted lines) optical functions. The spectral positions of the E_u ($\mathbf{E}\perp c$) and A_{2u} ($\mathbf{E}\parallel c$) phonon modes are indicated by brackets within the upper part of the graphs. The dotted brackets denote the LO phonons, and the solid brackets denote the TO phonons. The n and k optical functions provide important information about infrared absorption peak and phonon energies of sapphire substrate, and are critical references for subsequent numerical fitting about GaN/sapphire and

AlGa_xN/GaN/sapphire structures. The experimental (solid lines) and theoretical (dashed lines) infrared reflectance spectra of sapphire, GaN, AlN, and Al_xGa_{1-x}N epitaxial films with aluminum composition x from 0.15 to 0.58 are shown in Fig. 6. It is obvious that there is a sharp dip at 755 cm^{-1} in GaN and all Al_xGa_{1-x}N spectra compared with the spectra of sapphire. This dip is induced by LO phonon due to the optical anisotropy in the GaN material. Specifically, the p -polarized light of nonperpendicular incidence in the hexagonal epilayers can be interacted with the LO phonon mode and make it infrared active. For experimental reflectance spectra of Al_xGa_{1-x}N films, the incorporation of 15% aluminum results in an additional dip at about 648 cm^{-1} as compared with that of GaN. Moreover, the dip intensity increases with the dip position slight shift of toward higher frequency when the aluminum composition increases in the range from 0.15 to 0.58. The dip was also observed in the experimental reflectance spectra of Al_xGa_{1-x}N measured by Yu *et al.* [7]. They supposed the origin of this dip is related to the E_2 mode, which results from the random distribution of alloy constituents and the elimination of the translational symmetry of the lattice. In Fig. 6, it is found that when the aluminum composition is smaller than 0.24, the theoretical fitting reflectance spectra are in good agreement with experimental results. However, when the aluminum composition is 0.24, a new dip at about 785 cm^{-1} can be observed in the experimental reflectance spectrum. The dip intensity increases with increasing aluminum composition and the dip frequency shifts from 785 to 812 cm^{-1} as aluminum composition increases from 0.24 to 0.58. In order to further investigate the origin of this dip, the reciprocal space maps (RSMs) of x-ray diffraction intensity of Al_{0.2}Ga_{0.8}N and Al_{0.24}Ga_{0.76}N films were performed around an asymmetrical GaN ($10\bar{1}5$) Bragg peak as shown in Fig. 7. As depicted in Fig. 7 (a), the maximum of the Al_{0.2}Ga_{0.8}N reciprocal lattice points is at fully strained position. Since the layer thicknesses of all Al_xGa_{1-x}N

films are nearly the same, we assume that the lattice constant of $\text{Al}_x\text{Ga}_{1-x}\text{N}$ films with aluminum composition smaller than 0.2 is fully coherent to that of GaN bulk. Furthermore, when the aluminum composition of $\text{Al}_x\text{Ga}_{1-x}\text{N}$ films increases from 0.2 to 0.24, the maximum of the $\text{Al}_{0.24}\text{Ga}_{0.76}\text{N}$ reciprocal lattice points shifts from a fully strained to a partially relaxed position, as shown in Fig. 7 (b). The degree of strain relaxation shall progressively increase with increasing aluminum composition under the condition of similar AlGa_N layer thickness due to the large lattice mismatch between GaN and AlN. By comparing Fig. 6 and Fig. 7, it is found that the emergence of the dip at 785 cm^{-1} and the strain relaxation of AlGa_N film occur at the same aluminum composition. Moreover, the dip intensity increases with aluminum composition, which results in the increased degree of strain relaxation as well. Therefore, we deduce that the origin of this dip is attributed to the strain relaxation of $\text{Al}_x\text{Ga}_{1-x}\text{N}$ films. Since the phonon properties are closely related to the lattice vibration, crystal structure, and alloy composition, it can be expected that the fully strained, partially relaxed, and fully relaxed AlGa_N films shall eliminate the translational symmetry of the lattice, which influences the phonon properties and is characterized from the infrared reflectance spectra. It is reasonable that the measured infrared reflectance spectra of $\text{Al}_x\text{Ga}_{1-x}\text{N}$ films with aluminum composition larger than 0.24 cannot be excellently fitted by the symmetric physical model. The effect of strain relaxation of $\text{Al}_x\text{Ga}_{1-x}\text{N}$ films should be considered in the determination of phonon frequency since it is difficult to grow fully strained AlGa_N film with high aluminum composition. Since the samples were measured at a tilted angle, four phonon modes could be collected and analyzed.

The best fitting parameters of GaN/sapphire, and $\text{Al}_x\text{Ga}_{1-x}\text{N}$ /GaN/sapphire with aluminum composition from 0.15 to 0.24 are shown in Table 2. Since the fitting parameters of the reflectance spectra of $\text{Al}_x\text{Ga}_{1-x}\text{N}$ films with aluminum composition

larger than 0.24 are not reliable due to the mismatch between measured and calculated reflectance spectra, these parameters are not shown in Table 2. The anisotropic high-frequency dielectric constants $\epsilon_{\infty,\perp}$ and $\epsilon_{\infty,\parallel}$ decrease and the phonon frequency of ω_{TO} and ω_{LO} increase with increasing aluminum composition. The high-frequency dielectric constants of $\text{Al}_x\text{Ga}_{1-x}\text{N}$ decrease from 4.98 to 4.52, which are located between the values of 5.01 for $\text{Al}_{0.087}\text{Ga}_{0.913}\text{N}$ and 4.5 for $\text{Al}_{0.27}\text{Ga}_{0.73}\text{N}$. This result is not only important for future growth of the QCL structure but also is an important data for $\text{Al}_x\text{Ga}_{1-x}\text{N}$ materials. The results about infrared reflectance of optical phonon modes in AlGaN epitaxial layers grown on sapphire substrates have been published on SPIE proceeding paper in 2008 [8].

2.2 Growth and investigation of active region of quantum cascade laser

We have grown a multilayer structure of active region of GaN/AlGaN MQW structure which consists of 3 GaN QWs and 3 AlGaN barriers as shown in Fig. 8. This active region structure consists of 20 periods of MQW structure with each period consisting of 3 GaN/AlGaN QWs. Fig. 9 (a) shows a cross-sectional TEM image of the 20-period QC structure and each period consisting of 3 GaN QWs and 3 AlGaN barriers and (b) two periods of the QC structure. In Fig. 9(a), a contrast made by the periodically aligned 20 sets of the 3-period MQWs can be seen. In Fig. 9(b), bright parts and dark parts correspond to the AlGaN barriers and the GaN wells, respectively. From previous aluminum composition analysis in AlGaN material, we found that the aluminum composition of each layer was slightly off from the original design value as discussed in the last final report. A more precise control of the aluminum composition is needed for the active region structures to ensure proper operation of QCL.

In this year we started to investigate a new improved growth method, atomic layer deposition (ALD) method, which can provide a better control of the epitaxial layer thickness by near monolayer growth approach. Fig. 10 shows the sketch of atomic layer deposition of the GaN/AlN heterostructure. The ALD process involves alternate control of mass flow of trimethylaluminum and trimethylgallium gas during the growth of AlGaN barrier to form superlattice (SLs). The MO gas flow time of AlN and GaN layer were 6 and 19 sec respectively under a continuous flush of the NH₃ gas. The short interruption time was 10 sec between AlN and GaN. Under these growth conditions, the grown rate of ALD AlGaN is 0.14 μm/hr which is lower than the conventional growth rate of about 0.6 μm/hr~1 μm/hr. So the thickness can be well control by very low growth rate if using the ALD technique to grow it.

Using the ALD growth method, we have grown a test sample which has a three-quantum-well GaN/AlGaN structure as shown in Fig. 11. Fig. 12 shows a cross-sectional HRTEM image of the three-pair AlGaN/GaN quantum well structure. The insert image in Fig. 12 shows the enlarged MQWs schema and the scale bar is 5 nm. As shown in the Fig. 12, the ALD grown AlGaN barrier consists of six pairs of AlN/GaN superlattices with AlN thickness of 4.3 Å and GaN thickness of 7.7 Å respectively to form a AlGaN barrier thickness of 7.2 nm, while the GaN well has a thickness of 3 nm. The bright parts and dark parts correspond to the AlN and the GaN, respectively. The results show a clear image of interface and mono-atomic step indicating successful formation of superlattice by ALD process. Note that the interfaces of the AlGaN barriers on the GaN wells are as sharp as those of the GaN wells on the AlGaN barriers. This result indicates the ALD growth method can produce very controllable thickness in near monolayer scale better than the conventional growth method. In addition, we also observed that there are also no threading dislocations running across the MQW as

shown in the image. This suggests that the ALD method can also effectively suppress the penetration of thread dislocation through the MQW preventing the deterioration of the MQW.

We also investigated the HRXRD pattern of the grown sample. The $\omega/2\theta$ -scan (0002) reflections for AlGa_xN/GaN MQWs sample is shown in Fig. 13. The diffraction pattern shows the two periodical structures. One is the AlGa_xN/GaN MQWs, another is AlN/GaN SLs in the barrier of quantum well. The solid and dashed lines show the experimental and simulated results, respectively. The high order satellite peaks of QWs and SLs are clearly observed shown in Fig. 13(a). The five satellite peaks of QWs are from -3th to 2th. We also observed the -1 order peak of SLs. The separation of QWs and SLs satellite peak is 1.6 K and 9.0 K arcsec. These separations exhibit the thickness of periodical structure which indicates smooth and abrupt interfaces with good periodicity of the SLs and QWs structure. According to the simulation results, the six pairs of SLs structure have a thickness of 0.42 nm and 0.77 nm for AlN and GaN respectively forming an AlGa_xN barrier layer with an overall thickness of 7.14 nm. While the GaN well has a thickness of 2.9 nm. The result was similar to our HRTEM data in inserting graph of Fig. 12. In addition, the average Al content of AlGa_xN barrier is also estimated to be about 0.29. From the RSM data of AlGa_xN/GaN MQWs obtained from (10 $\bar{1}$ 5) diffraction shown in Fig. 13(b), the spread of RSM intensity for the AlGa_xN/GaN MQWs was relatively narrow indicating AlGa_xN epilayers exhibited relatively small distribution of crystal orientation. In addition, the reciprocal lattice points of AlGa_xN and GaN were lined up at the same Q_x position (red solid line) indicating the AlGa_xN and GaN had same lattice constant. According the earlier report, the degree of lattice relaxations can be estimated from the equation of $\epsilon_{xx} = q_x^{GaN} / q_x^{MQWs} - 1$, where the q_x^{GaN} and q_x^{MQWs} are the x position of GaN layer and AlGa_xN layer,

respectively. We obtained an estimated degree of lattice relaxation to be only 3.9×10^{-6} , indicating the AlGaN epilayer is fully strained and pseudomorphic to the underlying GaN layer. These results about atomic layer deposition have been published on SPIE proceeding paper in 2008 [9]. We are continuing the investigation of this subject during the new program phase and intend to submit a paper reporting new findings next year.

In summary, we have grown high crystalline quality AlGaN single layer and active region of GaN-based QCL by low-pressure MOCVD. The composition dependence of optical phonon energies were studied by Fourier transform infrared reflectance measurements and the phonon emission modes of AlGaN were clearly identified. We also conducted the preliminary investigation of growth of GaN/AlGaN quantum confine structures using atomic layer deposition method. Three pairs AlGaN/GaN MQWs by using AlN/GaN SLs as an AlGaN barrier layer was studied. From the HRTEM and HRXRD results, it shows the shape interface between SLs layers and QWs structure with good periodicity. For further understanding of the phonon properties of AlGaN material system, we will develop a physical model based on the data from FTIR in the next phase of the program. We will also continue to investigate the ALD growth method and to establish the optimal growth conditions to grow the full QCL structure for realization of the GaN/AlGaN QCL.

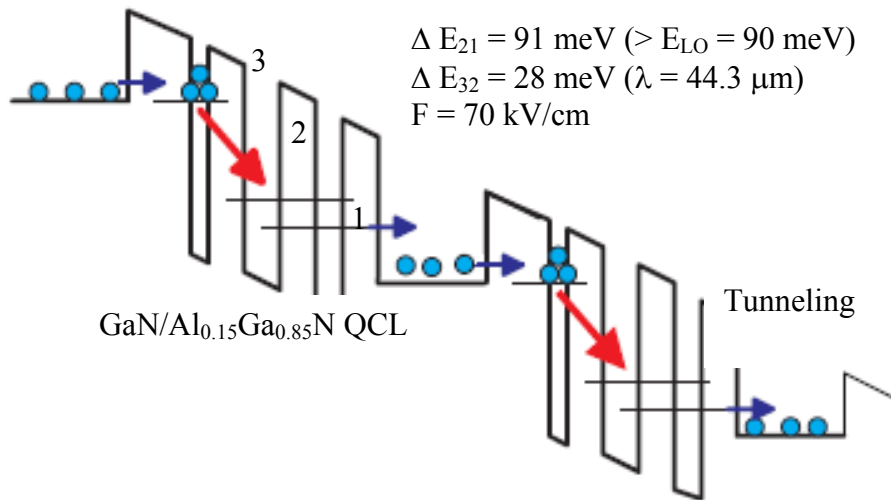


Fig. 1 Proposed GaN/AlGa_N QCL structure

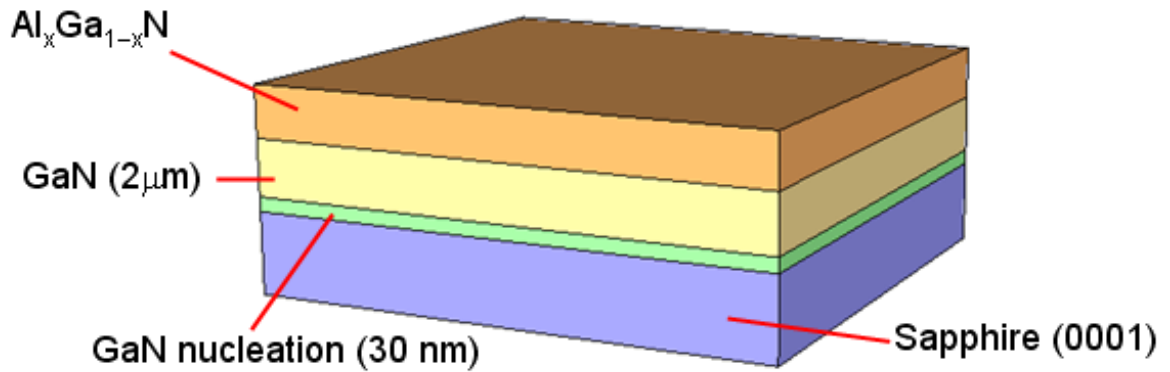


Fig. 2 Schematic diagram of the AlGa_N thin film grown with GaN buffer layer on the sapphire (0001).

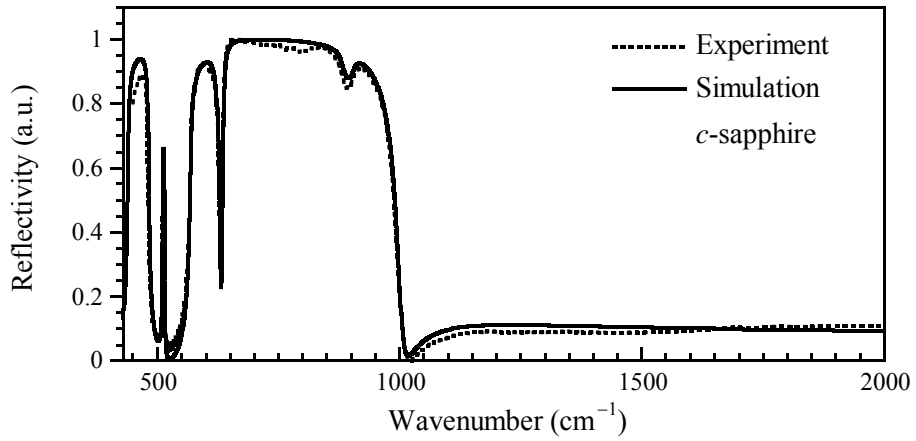


Fig. 3 Experimental (dotted line) and calculated (solid line) infrared reflectance spectra of the *c*-sapphire substrate.

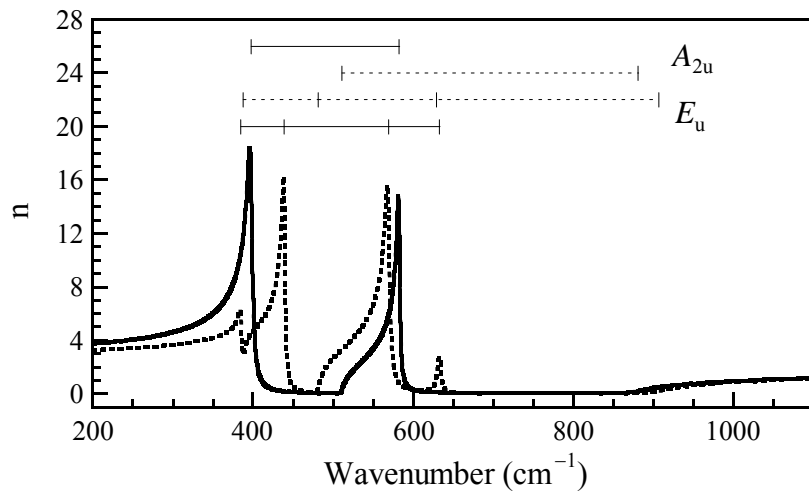


Fig. 4 Ordinary (solid line) and extraordinary (dotted line) refractive index for *c*-sapphire.

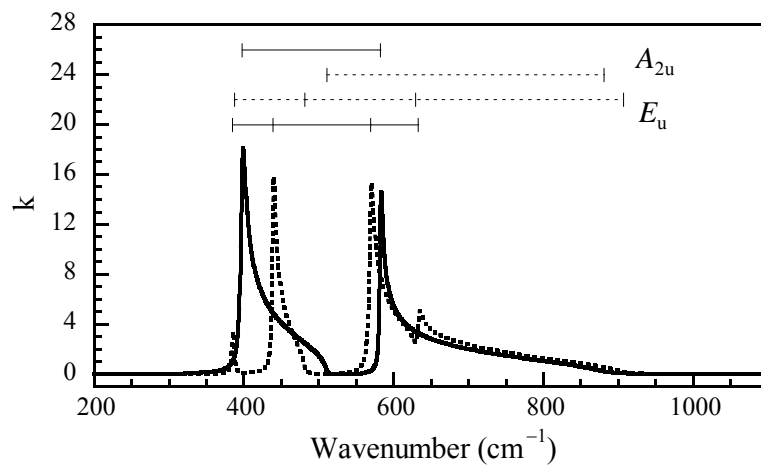


Fig. 5 Extinction coefficients of ordinary (solid line) ray and extraordinary (dotted line) ray for c-sapphire.

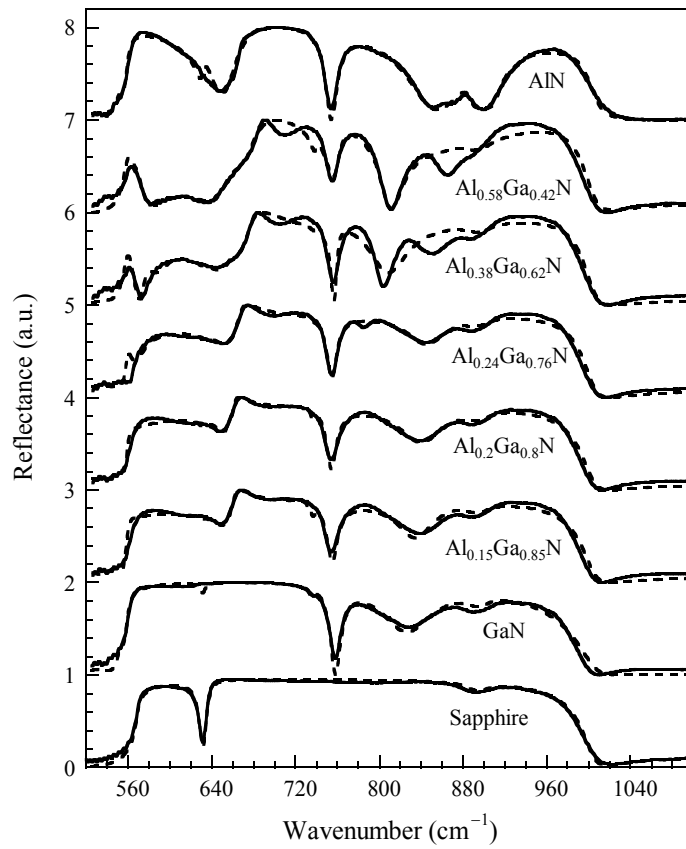


Fig. 6 Experimental (solid lines) and theoretical fitting (dashed lines) infrared reflectance spectra of sapphire, GaN on sapphire, and Al_xGa_{1-x}N films on sapphire with different aluminum compositions.

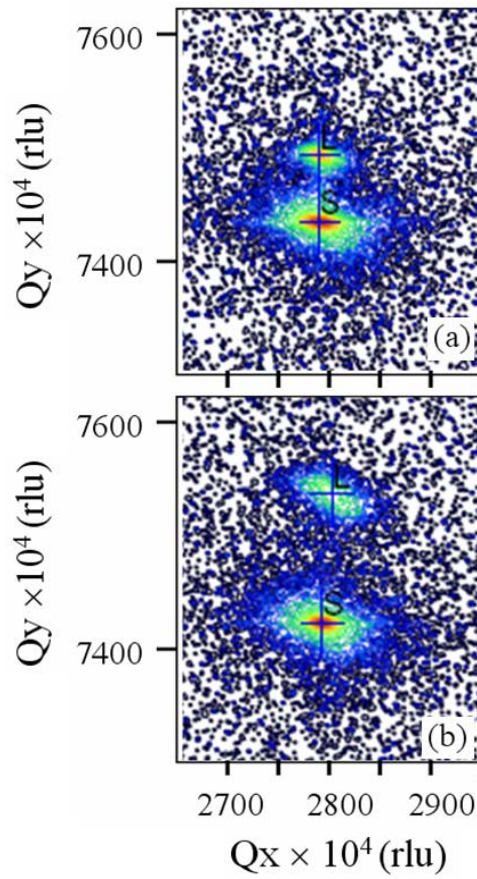


Fig. 7 Reciprocal space maps of (a) $\text{Al}_{0.2}\text{Ga}_{0.8}\text{N}$ and (b) $\text{Al}_{0.24}\text{Ga}_{0.76}\text{N}$ epitaxial films.

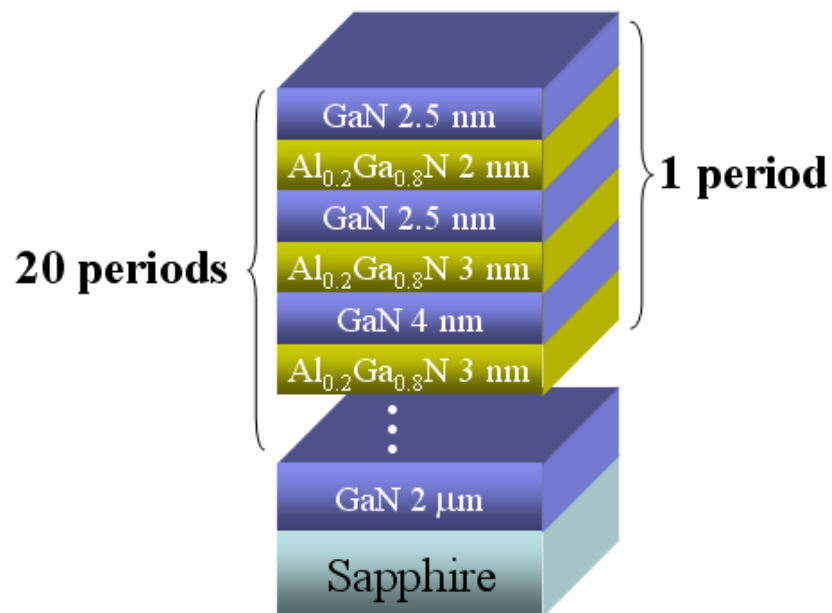


Fig. 8 Schematic of AlGaN QCL Active Layer Structure

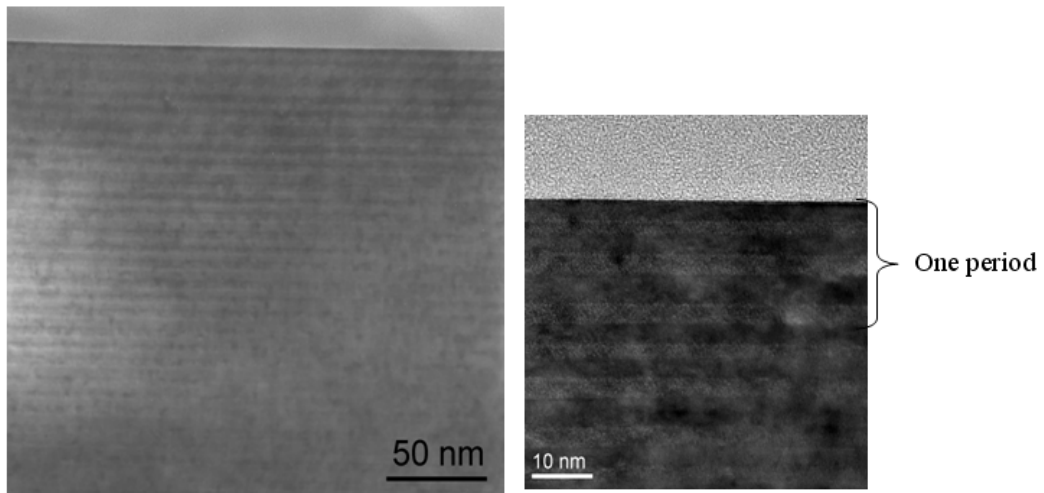


Fig. 9 Transmission electron microscope image of (a) the portion of the QCL structure and (b) two periods of QWs. Light grey layers indicate $\text{Al}_{0.15}\text{Ga}_{0.85}\text{N}$ and dark grey layers GaN.

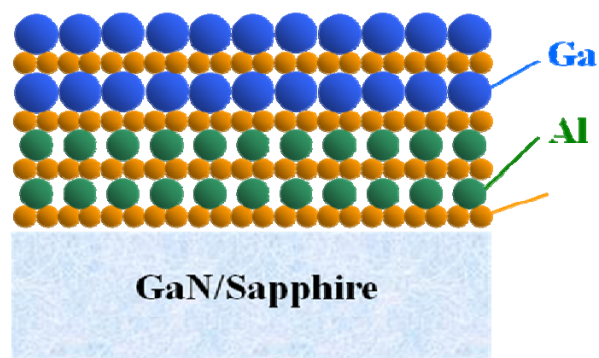


Fig. 10 Sketch of atomic layer deposition for GaN/AlN heterostructure.

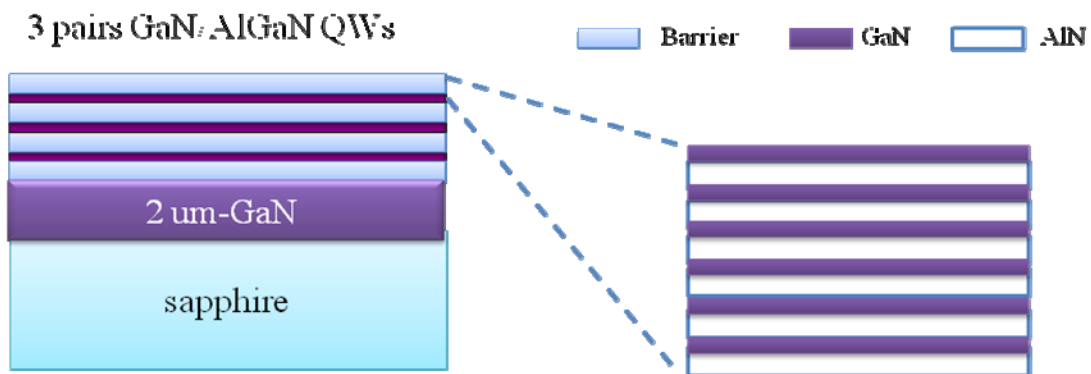


Fig. 11 Sketch of three pair AlGaN/GaN multiple quantum well grown by ALD technique in AlGaN barrier.

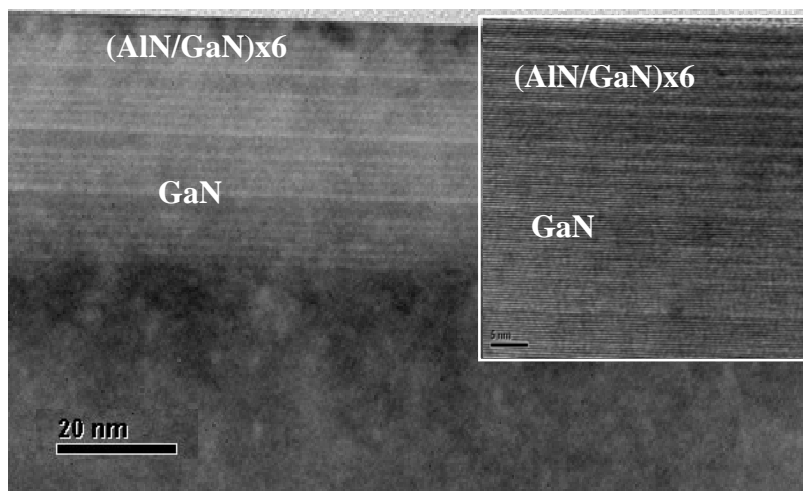


Fig.12 Transmission electron microscope image of the three pairs AlGaN/GaN multiple quantum well structure and the insert image is the part of the MQWs.

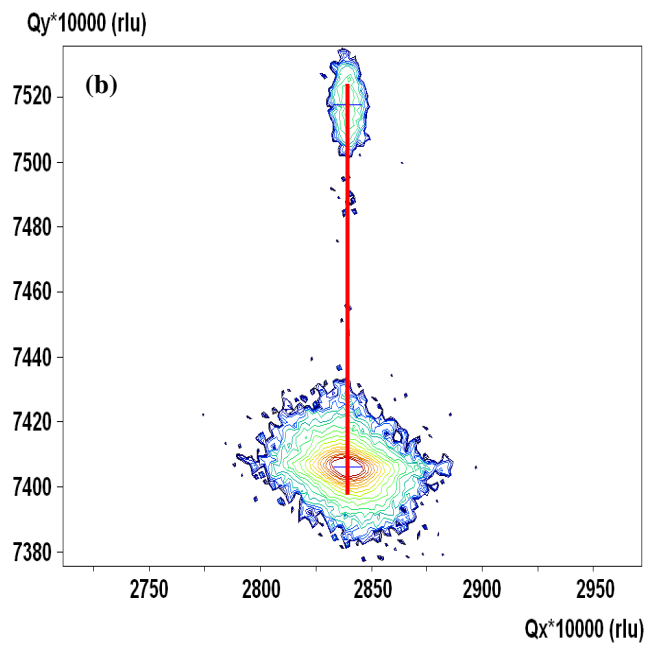
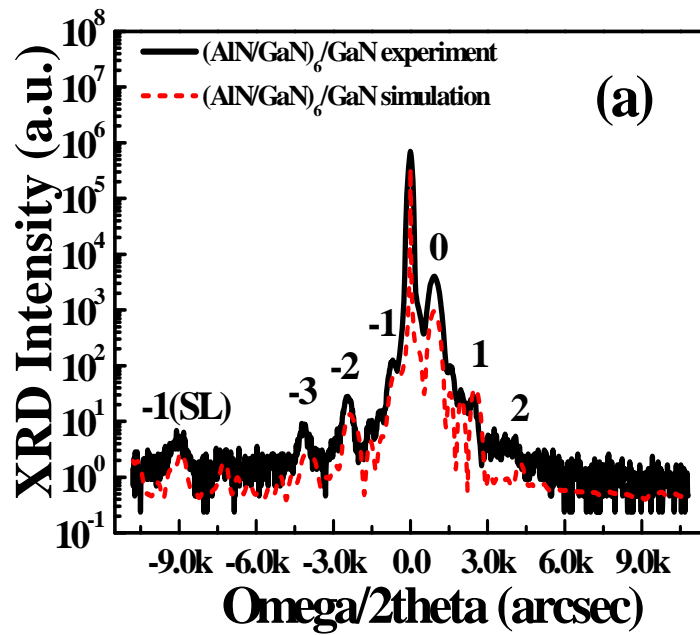


Fig. 13 (a) $(0\ 0\ 0\ 2)$ ω - 2θ x-ray diffraction pattern and simulated result of AlGa_N/Ga_N MQWs. The satellite peaks of QWs from the -3th to 2th. The -1th satellite peak of SLs is located at the -9.0 K from the Ga_N peak. (b) RSM of the sample obtained from $(1\ 0\ \bar{1}\ 5)$ diffraction.

Table. 1. Physical parameters of *c*-sapphire used in the calculation

	ϵ_∞	ω_{TO} (cm ⁻¹)	ω_{LO} (cm ⁻¹)	γ_{TO}	γ_{LO}
E_u	3.077	384.99	387.60	3.3	3.1
		439.10	481.68	3.1	1.9
		569.00	629.50	4.7	5.9
		633.63	906.60	5.0	14.7
A_{2u}	3.072	397.52	510.87	5.3	1.1
		582.41	881.10	3.0	15.4

Table. 2. Best fitting parameters of GaN/sapphire as well as Al_{*x*}Ga_{1-*x*}N/GaN/sapphire with aluminum composition from 0.15 to 0.24 determined by infrared reflectance spectra.

	GaN	Al _{0.15} Ga _{0.85} N	Al _{0.2} Ga _{0.8} N	Al _{0.24} Ga _{0.76} N
$\epsilon_{\infty,\perp}$	5.11	4.98	4.77	4.52
$\epsilon_{\infty,\parallel}$	5.07	4.95	4.65	4.50
$\omega_{\text{TO},\perp}$ (cm ⁻¹)	559.1	565.2	570.3	575.8
$\omega_{\text{TO},\parallel}$ (cm ⁻¹)	533.1	542.1	545.3	550.7
$\omega_{\text{LO},\perp}$ (cm ⁻¹)	742.2	775.1	787.6	790.2
$\omega_{\text{LO},\parallel}$ (cm ⁻¹)	734.5	762.1	775.8	780.6
$\omega_{\text{TO},\perp}$ (cm ⁻¹)		628.6	625.9	623.7
$\omega_{\text{TO},\parallel}$ (cm ⁻¹)		638.3	640.2	643.7

References

1. G. S. Huang, T. C. Lu, H. H. Yao, H. C. Kuo, S. C. Wang, "Crack-free GaN/AlN distributed Bragg reflectors incorporated with GaN/AlN superlattices grown by metalorganic chemical vapor deposition" *Appl. Phys. Lett.* **88**, 061904 (2006).
2. H. H. Yao, C. F. Lin, H. C. Kuo, S. C. Wang, "MOCVD growth of AlN/GaN DBR structures under various ambient conditions," *J. Crystal Growth* **262**, 151 (2004)
3. G. Sun, R. A. Soref, J. B. Khurgin, "Active region design of a terahertz GaN/Al_{0.15}Ga_{0.85}N quantum cascade laser," *Superlattice. Microstruct.* **37**, 107 (2005)
4. G. S. Huang, T. C. Lu, H. H. Yao, H. C. Kuo, S. C. Wang, G. Sun, C.-W. Lin, L. Chang, R. A. Soref, "GaN/AlGa_N active regions for terahertz quantum cascade lasers grown by low-pressure metal organic vapor deposition," *J. Crystal Growth* **298**, 687 (2007)
5. G. S. Huang, H. H. Yao, T. C. Lu, H. C. Kuo, and S. C. Wang, "Aluminum incorporation into AlGa_N grown by low-pressure metal organic vapor phase epitaxy," *J. Appl. Phys.*, **99**, 104901-1-104901-5, 2006.
6. M. Schubert, T. E. Tiwald, and C. M. Herzinger, "Infrared dielectric anisotropy and phonon modes of sapphire," *Phys. Rev. B*, **61**, 8187-8201, 2000.
7. G. Yu, H. Ishikawa, M. Umeno, T. Egawa, J. Watanabe, T. Soga, and T. Jimbo, "The infrared optical functions of Al_xGa_{1-x}N determined by reflectance spectroscopy," *Appl. Phys. Lett.*, **73**, 1472-1474, 1998.
8. Jun-Rong Chen, Tien-Chang Lu, Gen-Sheng Huang, Tsung-Shine Ko, Hao-Chung Kuo, and Shing-Chung Wang, August 2007, "Infrared reflectance of optical phonon modes in AlGa_N epitaxial layers grown on sapphire substrates", *Proceedings of SPIE*, Vol. 6894 (Gallium Nitride Materials and Devices III), pp. 68941U-1 -

68941U-9.

9. AlGa_N/Ga_N multiple quantum wells grown by atomic-layer deposition” by M. H. Lo, Z. Y. Li, J. R. Chen, T. S. Ko, T. C. Lu, H. C. Kuo, and S. C. Wang Proc. SPIE **6894**, 68941V (2008)